Indian Journal of Chemistry
Vol. 48A, April 2009, pp. 480-488

Photocatalytic behavior of CeO_2-TiO_2 system for the degradation of methylene blue

G Magesh, B Viswanathan*, R P Viswanath, T K Varadarajan

National Centre for Catalysis Research, Department of Chemistry, Indian Institute of Technology Madras, Chennai 600 036, India

Email: bvnathan@iitm.ac.in

Received 17 December 2008; revised and accepted 18 March 2009

Mixed oxide CeO_2-TiO_2 has been employed in the coupled semiconductor configuration for photocatalytic decomposition of methylene blue. This coupling has enabled decomposition with visible light while with pure TiO_2 only UV radiation can effect this decomposition. Synergy between the two oxides and the importance of adsorption in photocatalytic decomposition of MB are demonstrated.

Keywords: Semiconductors, Coupled semiconductors, Photocatalysis, Visible light photocatalysis, Methylene blue, Ceria, Titania

IPC Code: Int Cl.[8] B01J21/06; C01F17/00; C01G23/04

Protection of environment and renewable energy sources are the two major issues of concern worldwide. Photocatalysis is a promising process that can contribute in solving both these issues. A photocatalyst capable of utilizing sunlight to decompose the various pollutants present in air, water and surfaces can create a pollution-free world. In addition, a photocatalyst which can split water to produce hydrogen utilizing sunlight can contribute to the renewable energy source. TiO_2 is a widely used and studied photocatalyst because of its desirable properties like stability, low cost, favorable absorption of light, appropriate band positions and inertness. However, the bandgap of TiO_2 is large[1] and it can function only by absorbing UV light, whereas sunlight contains only < 10% UV radiation. For a catalyst to function using sunlight, it should absorb light in the visible region. This can be achieved by reducing the bandgap of available materials like TiO_2 by doping with various cations[1-6] or anions[7-9] or by coupling with other materials[10-12] having a lower bandgap. Various attempts have been made to reduce the bandgap of TiO_2 by doping various transition metal ions like V, Cr, Fe, Co, Ni and Cu. However conflicting results have been reported, with both increase[1-6] and decrease[13,14] in activity, when compared with TiO_2. Recently, studies dealing with rare earth elements like Ln, Nd, Eu and Ce mixed with TiO_2 showing activity in the visible region have been reported[15-27]. Rare earth elements mixed with TiO_2 show a red shift due to doping leading to the formation of inter band states[15,21]. Moreover, addition of rare earth element is found to reduce recombination of the electrons and holes effectively by trapping them as well as by facilitating their faster movement along the surface of TiO_2 [17,18,22]. Among the various rare earths, Ce has been reported to consistently show activity in visible region when mixed with TiO_2 [23-25]. The advantage associated with Ce is that it is one among the four most abundant rare earth elements. CeO_2 is widely used in fuel cells and pollution control applications because of its redox behavior, oxygen defects and catalytic activity[26,27]. Catalytic properties of CeO_2 have been attributed to the formation of Ce^{3+} defect sites and subsequent oxygen vacancies. CeO_2 is an n-type semiconductor whose bandgap has been reported to vary from 2.7-3.4 eV depending on the method of preparation[28]. In the present study, Ce ion modified TiO_2 has been prepared by a simple and economical route and its photocatalytic activity has been studied for the degradation of methylene blue (MB). A polyacrylamide gel route has been used to synthesize the nanoparticles of the catalyst[29-31]. With polymeric chains forming a network, metal ions are entrapped evenly within the polyacrylamide gel, which prevents the agglomeration of the particles.

Although various reports deal with visible light activity of Ce modified TiO_2, the mechanism has not yet been convincingly evolved. Understanding the mechanism involved in the observed visible light activity of Ce modified TiO_2 will be of help in developing further catalytic systems with still higher activity in the visible region.

Some reports claim that Ce, when doped into the lattice of TiO_2, leads to the formation of interband states resulting in photocatalytic activity when exposed to visible light[23,24]. However, the size difference between Ce (Ce^{4+} : 0.093 nm, Ce^{3+} : 0.103 nm) and titanium (Ti^{4+} : 0.068 nm) is large and Ce cannot be accommodated in the TiO_2 lattice.

The aim of this study is to explain the mechanism involved in the observed visible light activity of Ce ion modified TiO_2. In addition, previous reports claim that modifying TiO_2 with Ce ion will reduce the recombination of charge carriers because of the redox behavior exhibited by the Ce^{4+}/Ce^{3+} couple[23,24]. In such a case, Ce ion modified TiO_2 should have a higher activity than that of TiO_2 when the reactions are carried out in UV light alone. In order to confirm that Ce^{3+}/Ce^{4+} couple reduces the recombination rate, the reactions were also carried out in UV light.

Materials and Methods

Preparation and characterization of CeO_2–TiO_2

Nanoparticles of Ce ion modified TiO_2 were synthesized in an aqueous solution of polyacrylamide (mol. wt. 5000000, Otto kemi, India). The *p*H of the aqueous solution of polyacrylamide was adjusted to 12.7 using aqueous ammonia. Polyacrylamide was added during the catalyst preparation to limit the growth of the catalyst particles; the average size was 25 nm herein. Titanium(IV) isopropoxide (97%, Sigma Aldrich) and ammonium ceric nitriate (99.0%, SD Fine Chemicals, India) were taken as the source of titanium and cerium respectively. Titanium(IV) isopropoxide dissolved in dichloromethane (E. Merck, India) and ammonium ceric nitrate dissolved in doubly distilled water were added drop wise to the basic polyacrylamide solution at the rate of 1.5 ml per min and 0.5 ml per min respectively under vigorous stirring. The obtained gel was stirred for 12 h and then washed 3 times with doubly distilled water. It was then dried at 343 K and calcined in air for 6 h at 873 K. Various Ce loadings such as 0.25% (1 g catalyst = 0.025 g CeO_2 + 0.975 g TiO_2), 0.5%, 1.0%, 2.0%, 3.0%, 5.0% and 9.0% were prepared. Pure CeO_2 and TiO_2 were also prepared by the same method by precipitating only ammonium ceric nitrate and titanium (IV) isopropoxide, respectively under similar conditions as used for Ce modified TiO_2 preparation.

Cerium modified TiO_2, pure CeO_2, and TiO_2 were characterized by X-ray diffraction (XRD) (Rigaku D/max 2400 instrument, Ni-filtered Cu Kα radiation, λ = 1.5418 Å) and thermogravimetric analysis (TGA) (Perkin-Elmer TGA, Delta Series TGA 7) at a heating rate of 20ºC per min in air. Scanning electron microscopy (SEM) (FEI model: Quanta 200), transmission electron microscopy (TEM) (Philips CM12, 100 kV), and diffuse reflectance UV-visible spectroscopy (Varian Cary 5E) were used to characterize the morphology, size of the particles and absorption onset respectively. Degradation of methylene blue and colorimetric estimation of Ce were carried out using a Jasco V-530 UV-visible spectrophotometer.

Photocatalytic studies

Photocatalytic degradation of methylene blue (Loba Chemie, India) in visible light was carried out in a glass reactor (9 cm × 3.5 cm) with an outer jacket for water circulation. A sample of 0.1 g of the catalyst was suspended by stirring magnetically in 80 ml of 53.49×10^{-6} mol L^{-1} (42.79×10^{-7} mol / 80 ml) aqueous MB solution. The solution was stirred in dark for 30 minutes to attain the adsorption-desorption equilibrium and it was irradiated using a 400 W high pressure mercury lamp (ORIEL Corporation, USA) where light of wavelengths < 420 nm were cut off using a filter (HOYA L-42). The irradiation was carried out for 90 minutes. The samples were then centrifuged at 12,000 rpm to remove the suspended catalyst particles and then analyzed using UV-visible spectrophotometer after required dilution. The degradation of MB was monitored by measuring the absorbance at λ_{max} 662 nm. In another study, reactions were carried out in ultraviolet light in a photocatalytic apparatus with eight 8 W Hg lamps which emit only light of wavelength 365 nm using a quartz reactor (18 cm × 3.5 cm) under the same conditions i.e., concentration of MB, amount of catalyst, equilibration time, and irradiation time, as in visible light studies.

Adsorption and desorption studies

To study the reduction in concentration of MB due to its adsorption on catalyst surface, reactions were

also carried out in the dark under the same conditions as the irradiation reactions. Desorption experiments were carried out to confirm that all MB were adsorbed only on the catalyst surface. Desorption was done by separating the used catalyst from the reaction mixture by centrifugation followed by drying at 333 K. This was followed by sonicating the catalyst in dimethyl sulfoxide (DMSO) (E. Merck, India) for 30 min. followed by centrifugation to remove the catalyst. The process of sonicating the catalyst in DMSO followed by centrifugation was repeated two more times. The obtained clear solution was made upto known volume and analyzed by UV-visible spectrophotometry.

Colorimetric estimation of cerium

To estimate the exact amount of Ce loaded onto the various samples, colorimetric estimation of Ce was carried out[32,33]. Cerium ion in its oxidation state of 4+ has an absorption maximum at 320 nm. By monitoring the absorbance at 320 nm, the amount of Ce was estimated. This was carried out by dissolving the catalyst in hot conc. sulfuric acid. The resulting solution was diluted and all the Ce was oxidized to Ce^{4+} using potassium persulfate (E. Merck, India) as the oxidizing agent in presence of silver sulfate (CDH, India) as the catalyst. The resulting solution was boiled for 15 minutes to decompose the excess persulfate since persulfate also absorbs at 320 nm. Then the amount of cerium was estimated by UV-visible spectrophotometry.

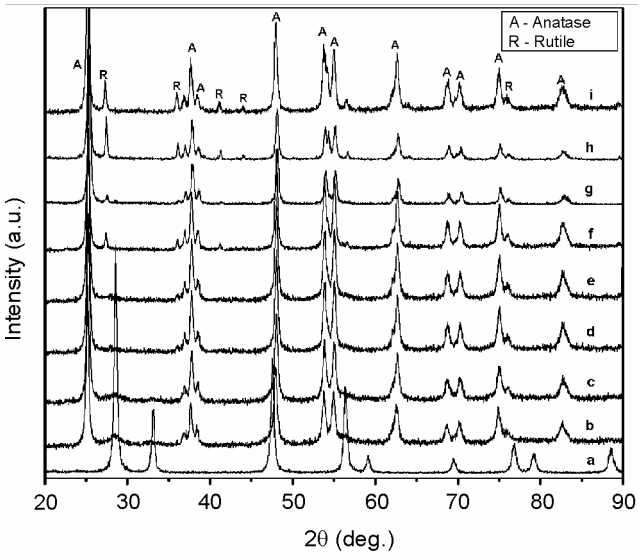

Fig. 1—X-ray diffraction patterns of CeO_2-TiO_2 samples. [(a) CeO_2; (b) 9% Ce-TiO_2; (c) 5% Ce-TiO_2; (d) 3% Ce-TiO_2; (e) 2% Ce-TiO_2; (f) 1% Ce-TiO_2; (g) 0.5% Ce-TiO_2; (h) 0.25% Ce-TiO_2; (i) TiO_2].

Results and Discussion

X-ray diffraction studies

X-ray diffraction patterns of all the prepared samples are given in Fig. 1. Ce-TiO_2 shows peaks corresponding to the presence of both anatase (JCPDS File No. 21-1272) and rutile (JCPDS File No. 21-1276) phases upto a Ce loading of 1%. At 2% loading of Ce (Fig. 1e) and above, the rutile peaks disappear and peaks due to cubic CeO_2 phase appear (Fig. 1b-d). This is in agreement with the reported ability of Ce to suppress the anatase to rutile phase transformation[34]. This is significant since anatase phase of TiO_2 is photocatalytically more active than rutile phase. Furthermore, this shows that the loaded Ce is present in the form of CeO_2 in the prepared catalyst. XRD patterns of all the samples, irrespective of the Ce loading, show line broadening which indicates the formation of nanoparticles. To further confirm the presence of CeO_2 in samples with low amounts of Ce, XRD measurements were performed for all the samples at a slow scan rate of 0.25° per min and 0.01° step size. The corresponding XRD patterns are given in Fig. 2, where the presence of CeO_2 peaks can be observed even at 0.5 and 1 % loading of Ce.

UV-visible spectra

UV-visible absorption spectra of TiO_2, CeO_2 and Ce modified TiO_2 are given in Fig. 3. From the onset of the absorption edge, the bandgap of the various samples were calculated using the method adopted by Tandon and Gupta[35]. UV-visible absorption spectrum shows an absorption onset at 400 nm for pure TiO_2

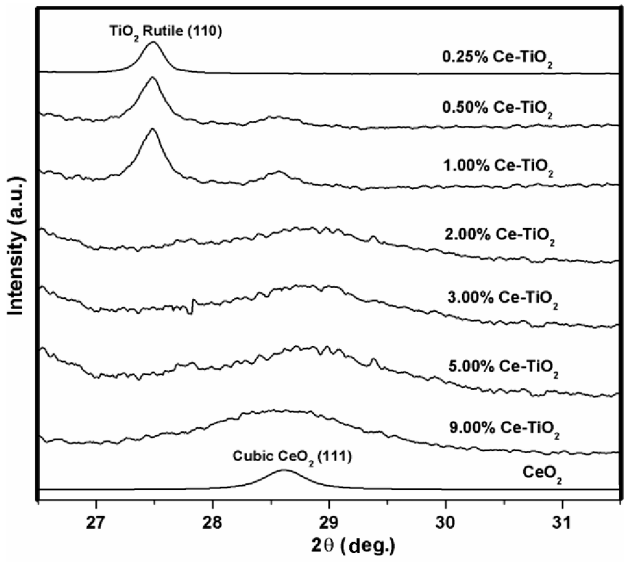

Fig. 2—XRD patterns of the samples scanned at a slow rate. [Scan rate= 0.3 degree per min].

and at 450 nm (bandgap = 2.76 eV) for pure CeO_2. Patsalas *et al*.[36] found that bandgap of CeO_2 varies and lower bandgap can be attributed to the presence of Ce^{3+} ions in the grain boundaries depending on the preparation method. Hence, the lower bandgap of CeO_2 in the prepared samples can be attributed to the presence of Ce^{3+} ions in the grain boundaries. For the Ce loaded TiO_2 samples, the absorbance shows a red shift with increase in the Ce loading which shows that CeO_2 is responsible for the observed shift in Ce modified TiO_2 samples. A red shift of upto 50 nm was observed for Ce loaded samples.

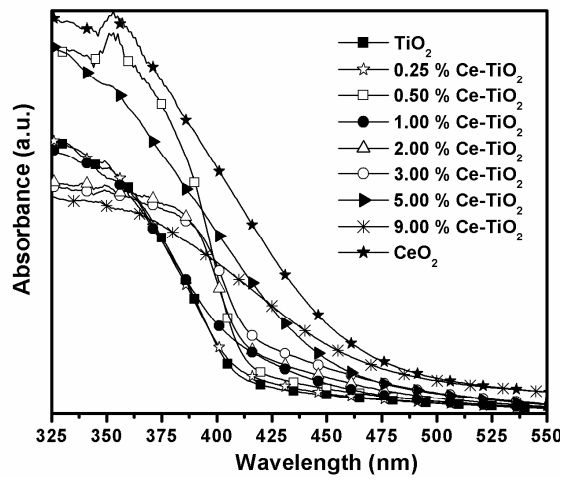

Fig. 3—UV-visible absorption spectra of the samples.

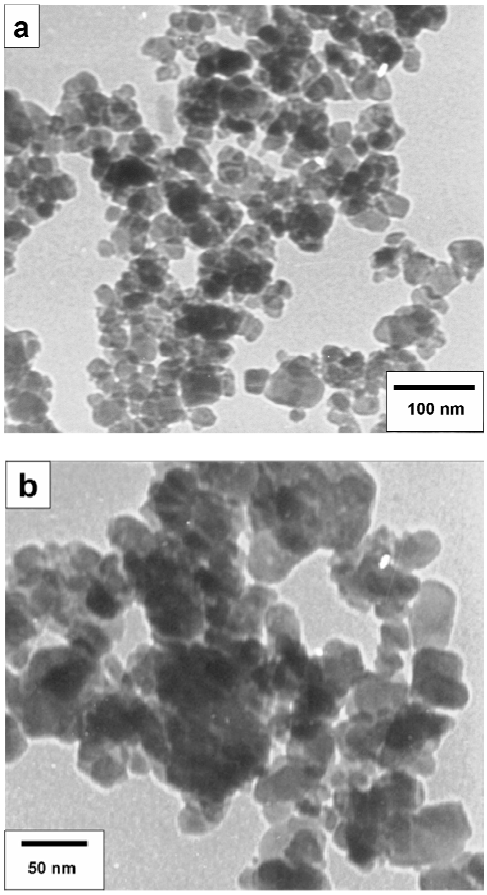

Fig. 4—TEM images of 3% Ce modified TiO_2. [(a) low magnification; (b) high magnification].

TEM and SEM analysis

TEM images of the Ce modified TiO_2 samples in different magnifications are given in Fig. 4. TEM analysis shows that nanoparticles do not have any specific shape. Particles are close to each other in the form of chains, which is typically observed in most of the reported microscopic images of TiO_2[37-39]. The particle sizes are distributed over a wide range (10-50 nm) and majority of the particles are 25 nm in size. SEM images of Ce modified TiO_2 samples are given in Fig. 5. Aggregates of particles measuring from 40 nm to 1 μm are observed in the SEM images.

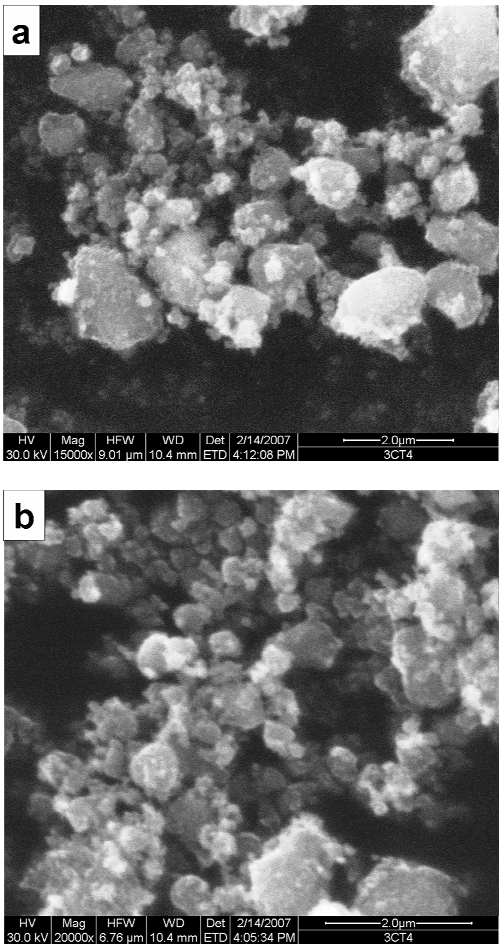

Fig. 5—SEM images of 3% Ce modified TiO_2. [(a) low magnification; (b) high magnification].

These aggregates are composed of the particles, which were observed in the TEM images. This is similar to that typically observed in previously reported images of TiO_2 [40]. This is due to the fact that the particles are well dispersed by sonication in acetone before taking TEM images.

TGA and elemental analyses

The TGA profile of as-synthesized TiO_2 shows weight loss upto 723 K which can be attributed to the decomposition of the polyacrylamide. Based on this observation, the samples were calcined at 873 K for 6 h in air. Energy Dispersive X-ray (EDX) spectrum of Ce modified TiO_2 confirms the presence of titanium, oxygen and cerium in the prepared oxides. Percentage of cerium estimated by colorimetry is given in Table 1. The results are well in agreement with the cerium taken in the precursor.

Adsorption and photocatalytic studies in visible light

The overall decrease in the concentration of MB under visible light irradiation is presented in Table 2. Considerable decrease in concentration was observed in the case of pure TiO_2 which does not show visible light absorption. In order to check whether adsorption of MB on the photocatalyst has a role in the decrease in concentration, reactions were carried out in the absence of irradiation, under similar conditions as that under irradiation. Reactions carried out in dark help in establishing the reaction mechanism involved as well. Table 3 shows the concentration of MB adsorbed on the catalyst in the absence of irradiation. It can be seen that reduction in the concentration of MB under dark, in the case of pure TiO_2, is the same as that under irradiation conditions. Moreover, the concentration of MB adsorbed was found to decrease with increasing concentration of CeO_2. The reason for adsorption could be as follows: methylene blue, which chemically is 3,7-bis(dimethylamino)phenazathionium chloride trihydrate, has a positively charged sulfur atom. Electrophoresis experiments show that MB remains positive in the *p*H range 4-9 (ref. 41). TiO_2 in aqueous solutions has a Point of Zero Charge (PZC) of 6, so that at *p*H > 6, the surface of TiO_2 becomes negatively charged. Since the reactions are carried out in neutral medium, positively charged MB is adsorbed on negatively charged surface of TiO_2 by electrostatic attraction[41-43]. To further confirm that MB is adsorbed on TiO_2 by purely electrostatic interactions, desorption experiments were carried out by dispersing the catalyst in a more polar solvent, DMSO, results of which are presented in Table 3. It can be seen that almost all the MB adsorbed on the catalyst is recovered during desorption experiments. The studies further show that adsorption of MB on TiO_2 is 3 times more as compared to that on CeO_2.

The decrease in MB concentration solely due to photocatalytic degradation is thus obtained by subtracting the concentration of MB adsorbed from

Table 1—Colorimetric estimation of Ce^{4+} in the mixed oxides

Amt of Ce^{4+} loaded (%)	Amt of Ce^{4+} estimated (%)
0.25	0.23
0.50	0.46
1.00	0.93
2.00	1.87
3.00	2.84
5.00	4.70
9.00	8.55

Table 2—Overall and net photocatalytic reduction in concentration of MB under UV and visible light irradiation after 90 minutes

Catalyst	Amt reduced ($\times 10^{-7}$ mol/0.1 g cat.)			
	Visible		UV	
	Overall	Net photo-catalytic	Overall	Net photo-catalytic
TiO_2	9.63	0.53	32.40	23.30
0.25 % Ce-TiO_2	14.65	6.31	34.56	26.22
0.50 % Ce-TiO_2	17.01	9.74	37.28	30.01
1.00 % Ce-TiO_2	16.80	10.27	40.45	33.92
2.00 % Ce-TiO_2	14.65	8.87	39.22	33.44
3.00 % Ce-TiO_2	14.12	8.66	31.61	26.18
5.00 % Ce-TiO_2	11.34	6.74	28.17	23.57
9.00 % Ce-TiO_2	9.73	5.55	26.83	22.65
CeO_2	8.66	5.24	5.18	1.76

Table 3—Amount of MB adsorbed in dark after 90 minutes of stirring and MB desorbed from used catalyst using DMSO

Catalyst	Amt adsorbed ($\times 10^{-7}$ mol / 0.1 g cat.)	Amt desorbed ($\times 10^{-7}$ mol / 0.1 g cat.)
TiO2	9.10	8.55
0.25 % Ce-TiO_2	8.34	7.81
0.50 % Ce-TiO_2	7.27	6.74
1.00 % Ce-TiO_2	6.53	5.88
2.00 % Ce-TiO_2	5.78	5.46
3.00 % Ce-TiO_2	5.46	4.82
5.00 % Ce-TiO_2	4.60	4.28
9.00 % Ce-TiO_2	4.18	3.74
CeO_2	3.42	3.10

the overall decrease in concentration (Table 2). It can be seen that the photocatalytic degradation of MB increases with increasing Ce amounts up to 1%, beyond which the concentration of MB degraded was found to decrease. It is important to note that the photoactivity of all Ce modified TiO_2 samples are higher than that of pure TiO_2 and CeO_2, indicating that Ce and TiO_2 have a synergistic effect in the photodegradation of MB.

Mechanism for visible light activity

There are two possible mechanisms for the observed visible light photocatalytic activity of the Ce modified TiO_2. Firstly, the substitution of Ce into the TiO_2 lattice leading to the formation of mixed oxides. This may result in the formation of additional energy states belonging to partially filled Ce 4*f* levels between the conduction and valence band (VB) of TiO_2. Visible light can excite the electrons from the VB to the interband Ce 4*f* levels or from the Ce 4*f* levels to the conduction band (CB) leading to the formation of electrons and holes. Formation of mixed oxides of Ce and Ti can be revealed by studying the XRD patterns. There are six phases of mixed oxides which are reported in the JCPDS database. X-ray diffractions patterns for the prepared Ce modified TiO_2 show no peaks corresponding to any of these six phases of Ce-Ti mixed oxides even at the highest loading of 9% of Ce. In addition, doping of Ce into the lattice of TiO_2 should lead to an increase in *d*-values between the corresponding planes. The calculated *d*-values for both the anatase and rutile peaks (Fig. 1) of the various Ce modified TiO_2 are found to be the same as that of pure TiO_2. This can be attributed to the absence of mixed oxides of Ce and Ti in the prepared Ce modified TiO_2 samples. Doping of Ce into TiO_2 lattice is not possible due to the fact that Ce and Ti have different coordination numbers of 8 and 6 in CeO_2 and TiO_2 respectively. It is difficult for the 8 coordinated Ce present in cubic CeO_2 lattice to replace 6 coordinated Ti in tetragonal TiO_2 lattice[35]. Further, the ionic size of Ce^{4+} and Ti^{4+} are 0.093 nm and 0.068 nm, respectively; the difference in ionic radius being high, lattice substitution in TiO_2 by Ce^{4+} is highly improbable. This shows that Ce is present as CeO_2 on the surface of TiO_2[34].

The second mechanism which can explain the observed visible light activity is the coupled semiconductor mechanism. Band energy positions of the various oxides involved like CeO_2, Ce_2O_3 and TiO_2 are required to establish the coupled semiconductor mechanism. To calculate the band positions of CeO_2, we have followed the same method used by Xu & Schoonen[44]. This method has been verified for more than 30 metal oxides and sulfides and found to be well in agreement with the experimentally determined values. This method is based on the concept that electronegativity of a compound is the geometrical mean of the electronegativity of the various elements involved. The electronegativity, electron affinity (EA), and ionization energy (IE) values of the compound are equivalent to that of the Fermi level energy, CB energy, and VB energy respectively. By adding and subtracting half of the bandgap value (i.e., $E_g/2$) from the electronegativity of the compound, the VB energy (IE) and CB energy (EA) respectively of the compound can be calculated using Eqs 1 and 2.

$$IE(TiO_2) = E_{VB}(TiO_2) = \chi\,(TiO_2) + \tfrac{1}{2}\,Eg \quad \ldots\ (1)$$

$$EA(TiO_2) = E_{CB}(TiO_2) = \chi\,(TiO_2) - \tfrac{1}{2}\,Eg \quad \ldots\ (2)$$

where E_g, EA, IE, E_{CB}, and E_{VB} represent the bandgap, electron affinity, ionization energy, conduction band energy position and valence band energy position of the compound respectively. The values obtained which are in absolute vacuum scale (AVS), can be converted to the normal hydrogen electrode (NHE) scale by subtracting 4.5 from the AVS values.

$$E_{CB}(TiO_2)_{\text{(in NHE)}} = E_{CB}(TiO_2) - 4.5\ \text{eV}_{\text{(in AVS)}}$$

The energy values of the bands calculated based on the above equation are listed in Table 4. The calculated energy position values show that both the oxides of Ce, i.e., CeO_2 and Ce_2O_3, have CB energies more negative than that of TiO_2. It is clear from the recorded UV-visible spectrum (Fig. 3) and literature reports[44] that CeO_2 and Ce_2O_3 have bandgaps which can absorb light in the visible region upto 450 nm and 516 nm respectively.

Since CeO_2 and Ce_2O_3 absorb light in the visible region and have CB energy more negative than that of TiO_2, they will transfer excited electrons to the CB of TiO_2. Ce_2O_3 is an unstable compound and gets

Table 4—Band gap, conduction and valence band energy positions of the various oxides

Semiconductor	Band gap (eV)	E_{CB} in NHE (eV)	E_{VB} in NHE (eV)
TiO_2	3.20	-0.29	2.91
CeO_2	2.76	-0.32	2.44
Ce_2O_3	2.40	-0.47	1.93

oxidized to CeO_2 in presence of trace amounts of O_2. Even though the presence of Ce_2O_3 has not been confirmed it may exist in aqueous medium under the photocatalytic reactions conditions. The electrons present on CB of TiO_2 will then be used for the various processes leading to formation of hydroxyl radicals which will then oxidize the adsorbed MB. In the case of CeO_2 even though it can form the oxidizing species like hydroxyl radicals, availability of MB on CeO_2 surface is less as compared to that on TiO_2 (Table 3). Thus the hydroxyl radicals formed through CB of CeO_2 get recombined to form H_2O_2 or react with other species without oxidizing the MB. Since the excited electrons in CeO_2 are immediately transferred to TiO_2, the recombination of charge carriers is significantly reduced in the coupled CeO_2-TiO_2 compared to pure CeO_2. A representation of the coupled semiconductor mechanism responsible for visible light activity is given in Scheme 1.

However, it is assumed that visible light induced degradation of MB is small, since the absorption wavelength required for MB is 608 nm and 662 nm. Previous reports also show very little reduction in MB under photolysis. Madhavi *et al.*[45] reported a 12% degradation of methylene blue under UV + visible light photolysis whereas 100% degradation can be achieved in presence of catalyst under same conditions. This shows that the observed degradation of methylene blue is due to the photocatalytically generated electrons and holes and not due to the self degradation of methylene blue.

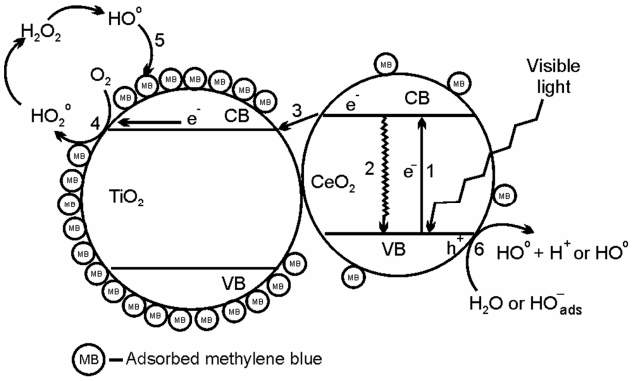

Step 1 - Excitation of CeO_2 by visible light
Step 2 - Recombination of charge carriers
Step 3 - Transfer of excited e^- to CB of TiO_2
Step 4 - Transfer of electron from CB of TiO_2 to dissolved O_2
Step 5 - Oxidation of MB by hydroxyl radicals
Step 6 - Oxidation of H_2O and HO^- to HO° by holes

Scheme 1

Optimum loading of cerium

Photocatalytic activity in visible light among the various Ce modified TiO_2 catalysts as compared to TiO_2 increases when 0.25% Ce is loaded and reaches a maximum with 1.0% Ce loading. Further loading decreases the activity and at 9% Ce loading, the activity is equal to that of CeO_2. This can be explained as follows: Cerium in Ce modified TiO_2 is uniformly dispersed on the TiO_2 surface in the form of CeO_2. CeO_2 can absorb visible light and then transfer the excited electrons to TiO_2 whereas TiO_2 can adsorb MB efficiently. At 0.5% and 1.0% loading of Ce, the coverage of TiO_2 surface by CeO_2 is optimum so that enough CeO_2 can be in contact with TiO_2. Also, there is enough uncovered surface of TiO_2 where MB can get adsorbed. This leads to a situation where absorption of light by CeO_2 forming excited electrons and holes, transfer of electrons to TiO_2, adsorption of MB on TiO_2, and the oxidation of MB by hydroxyl radicals are taking place simultaneously in an optimum manner. When the loading of Ce is increased, more CeO_2 has covered the surface of TiO_2 and lesser surface of TiO_2 is in contact with the MB solution. Thus even though the absorption of light by CeO_2 increases, the adsorption of MB by TiO_2 decreases due to lowering of the available surface area, hampering the reaction of MB with the hydroxyl radicals. Ce modified TiO_2 (2-5%) catalysts still give a higher activity than pure TiO_2 but less than 1% Ce modified TiO_2. At a loading of 9% of Ce, the surface is almost fully covered by CeO_2 and even though there is enough visible light absorption there is very little adsorption of MB on TiO_2. Thus, 9% cerium loaded samples gives almost the same activity as that of pure CeO_2.

Optimum loading can also be attributed to the higher reduction in recombination while there is 1% Ce on TiO_2. When there is a thin layer of CeO_2 present on the surface of TiO_2, the excited electrons created in CeO_2 due to visible light irradiation can be immediately transferred to TiO_2. This leads to an efficient separation of the electrons and holes across the boundary between TiO_2 and CeO_2 thereby reducing the recombination. Above the optimum loading of CeO_2, the thickness of CeO_2 layer becomes higher, and the electrons and holes created on the CeO_2 at the surface get recombined before the electrons travel and reach the CeO_2-TiO_2 interface. These results demonstrate that the poor visible light photocatalytic activity of CeO_2 inspite of having a

suitable bandgap and band position is because of very high recombination as well as poor adsorption towards MB. However, it should be remembered that CeO_2 shows far better activity in visible light compared to pure TiO_2.

Photocatalytic activity in UV light

There are some reports which claim that the Ce^{3+}/Ce^{4+} redox couple can reduce the recombination by enabling faster electron transfer along the TiO_2 surface[34, 46]. Since increase in activity of Ce modified TiO_2 in visible light can be attributed to the coupled semiconductor mechanism, we have carried out the reactions using only UV light to study the effect of Ce^{3+}/Ce^{4+} couple in reducing recombination. The results are tabulated in Table 2. In this case also, the net reduction in concentration due to photocatalysis is calculated by subtracting the concentration reduced due to adsorption from the overall reduction in concentration under UV light irradiation. The results show that modifying TiO_2 with Ce considerably enhanced activity in the UV light as well. Even with 0.25% Ce loading, an increase in activity as compared to that of pure TiO_2 is observed. The optimum Ce loading was found to be between 0.5-2.0%. With further increase in Ce loading the activity was found to decrease and was found to be less than that of pure TiO_2. Pure CeO_2 showed negligible activity in UV light. These observations can be explained as follows: The reduction of Ce^{4+} to Ce^{3+} requires a potential of +1.61 V (vs NHE) and oxidation of Ce^{3+} to Ce^{4+} requires -1.61 V (vs NHE). The CB of TiO_2 has a potential of – 0.29 V which is more negative than that of Ce^{4+} to Ce^{3+} reduction potential. Hence, the CB electrons of TiO_2 are able to reduce Ce^{4+} to Ce^{3+}. Also, the VB of TiO_2 has a potential of + 2.91 V which is more positive than Ce^{3+} to Ce^{4+}oxidation potential. The VB electrons can hence oxidize Ce^{3+} to Ce^{4+}. These reduced Ce^{3+} and oxidized Ce^{4+} species can subsequently transfer the charges to the species present in the reaction medium[18]. Hence, the Ce ions reduce the recombination of the charge carriers enhancing the activity in the UV light as well. The reason for the observed optimum loading in this case can be attributed to CeO_2 being less active than TiO_2. Below 3% Ce loading, the amount of Ce^{4+}/Ce^{3+} present on the TiO_2 surface is favorable for faster charge transfer and at the same time allows light to reach the TiO_2 surface. However, above 3% Ce loading the amount of CeO_2 on the surface of TiO_2 is very high such that it blocks absorption of light by TiO_2 showing lesser activity than that of pure TiO_2.

Conclusions

Ce modified TiO_2 nanoparticles have been prepared by a simple polymer assisted method. The prepared Ce modified TiO_2 samples show red shift as compared to TiO_2 in UV-visible spectrophotometry and are active in visible light for the photocatalytic degradation of MB with 0.1% Ce-TiO_2 showing the highest activity. The mechanism of visible light photocatalytic activity has been established. Added Ce is present as CeO_2 on the surface of TiO_2 and its CB energy is more negative than that of TiO_2. CeO_2 absorbs visible light and transfers the excited electrons to CB of TiO_2 which has been utilized for the photocatalytic degradation of MB. CeO_2 having a suitable band gap and band position is less active in visible light than Ce modified TiO_2 because of high recombination and poor adsorption of MB. Higher amount of Ce loading leads to a decrease in activity because of the blocking of TiO_2 surface by CeO_2 as well as due to increase in recombination of charge carriers. Reactions in UV light confirm that Ce loading reduces the recombination of charge carriers because of the easy redox nature of Ce^{4+}/ Ce^{3+} couple. Although red shift in Ce modified TiO_2 is less, insights obtained in this study will be helpful in developing coupled semiconductor photocatalysts. Moreover, the importance of adsorption in determining the photocatalytic activity shows that it should be considered while selecting the photocatalysts for different target compounds. This study also shows that coupling a photocatalyst with high recombination rate to a suitable material will enhance its activity.

Acknowledgement

We thank the Department of Science and Technology (DST), New Delhi, for funding the research and fellowship to one of the authors (GM). The funding from DST for NCCR is also gratefully acknowledged.

References

1 Klosek S & Raftery D, *J Phys Chem B*, 105 (2002) 2815.
2 Shi J Y, Leng W H, Zhu W C, Zhang J Q & Cao C N, *Chem Eng Technol*, 29 (2006) 146.
3 Zhu J, Deng Z, Chen F, Zhang J, Chen H, Anpo M, Huang J & Zhang L, *Appl Catal B*, 62 (2006) 329.
4 Zhu J, Zheng W, He B, Zhang J & Anpo M, *J Mol Catal A: Chem*, 216 (2004) 35.

5 Kim D H, Hong H S, Kim S J, Song J S & Lee K S, *J Alloys Comp*, 375 (2004) 259.
6 Morikawa T, Irokawa Y & Ohwaki T, *App Catal A*, 314 (2006) 123.
7 Yamaki T, Sumita T & Yamamoto S, *J Mater Sci Lett*, 21 (2002) 33.
8 Sathish M, Viswanathan B, Viswanath R P & Gopinath C S, *Chem Mater*, 17 (2005) 6349.
9 Sathish M, Viswanathan B & Viswanath R P, *Appl Catal B*, 74 (2007) 307.
10 Bassekhouad Y, Chaoui N, Trzpit M, Ghazzal N, Robert D & Weber J V, *J Photochem Photobiol, A*, 183 (2006) 218.
11 Wu L, Yu J C & Fu X, *J Mol Catal A: Chem*, 244 (2006) 25.
12 Ho W & Yu J C, *J Mol Catal A : Chem*, 247 (2006) 268.
13 Cameiro J O, Teixeira V, Portinha A, Magalhaes A, Newton R & Coutinho P, *Mat Sci Eng B*, 138 (2007) 144.
14 Chang J T, Lai Y F & He J L, *Surf Coat Technol*, 200 (2005) 1640.
15 Xie Y &Yuan C, *Appl Surf Sci*, 221 (2004) 17.
16 Xie Y, Yuan C & Li X, *Coll Surf, A*, 252 (2005) 87.
17 Xie Y &Yuan C, *Mater Res Bull*, 39 (2004) 533.
18 Xie Y, Yuan C & Li X, *Mater Sci Eng, B*, 117 (2005) 325.
19 Wei H, Wu Y, Lun N & Zhao F, *J Mater Sci*, 39 (2004) 1305.
20 Liu H & Gao L, *Chem Lett*, 33 (2004) 730.
21 Li F B, Li X Z & Cheah K W, *Environ Chem*, 2 (2005) 130.
22 Li F B, Li X Z, Ao C H, Lee S C & Hou M F, *Chemosphere*, 59 (2005) 787.
23 Tong T, Zhang J, Tian B, Chen F, He D & Anpo M, *J Coll Interface Sci*, 315 (2007) 382.
24 Pavasupree S, Suzuki Y, Pivsa-Art S & Yoshikawa S, *J Solid State Chem*, 178 (2005) 128.
25 Liu B, Zhao X, Zhang N, Zhao Q, He X & Feng J, *Surf Sci*, 595 (2005) 203.
26 Nolan M, Parker S C & Watson G W, *J Phys Chem B*, 110 (2006) 2256.
27 Carrettin S, Concepcion P, Corma A, Lopez J M N & Puntes V F, *Angew Chem Int Ed*, 43 (2004) 2538.
28 Ozer N, *Sol Energy Mater Sol Cells*, 68 (2001) 391.
29 Douy A & Odier P, *Mater Res Bull*, 24 (1989) 1119.
30 Pal A, Shah S & Devi S, *Colloids Surf, A*, 302 (2007) 51.
31 Pan C, Li X, Wang F & Wang L, *Ceram Int*, 34 (2008) 439.
32 Kolthoff I M, Elving P J & Sandell E B, *Treatise on Analytical Chemistry,* Part II, Vol 8 (Interscience Publishers, New York) 1963.
33 E.B. Sandell, *Colorimetric Determination of Traces of Metals,* 3rd Edn, (Interscience Publishers, London) 1959.
34 Xu Y, Chen H, Zeng Z & Lei B, *App Surf Sci*, 252 (2006) 8565.
35 Tandon S P & Gupta J P, *Phys Status Solidi*, 38 (1970) 363.
36 Patsalas P, Logothetidis S, Sygellou L & Kennou S, *Phys Rev B: Conden Matter*, 68 (2003) 35104.
37 Yang Y, Ma J, Qin Q, Zhai X, *J Mol Catal A: Chem*, 267 (2007) 41.
38 Zhang D R, Kim Y H, Kang Y S, *Curr Appl Phys*, 6 (2006) 801.
39 Park O K & Kang Y S, *Coll Surf, A*, 257 (2005) 261.
40 Mashid S, Askari M & Ghamsari M S, *J Mater Process Technol*, 189 (2007) 296.
41 Fetterolf M L, Patel H V & Jennings J M, *J Chem Eng Data*, 48 (2003) 831.
42 Chuan X Y, Hirano M & Ingaki M, *Appl Catal, B*, 51 (2004) 255.
43 Chen F, Zhao J & Hidaka H, *Res Chem Intermed*, 29 (2003) 733.
44 Xu Y & Schoonen M A A, *Am Mineral*, 85 (2000) 543.
45 Madhavi S & Tim W, *Environ Sci Technol*, 41 (2007) 4405.
46 Li F B, Li X Z, Hou M F, Cheah K W & Choy W C H, *App Catal A*, 285 (2005) 181.